ENCIT 2018

ABCM Associação Brasileira de Engenharia e Ciências Mecânicas

17th Brazilian Congress of Thermal Sciences and Engineering
November 25th-28th, 2018, Águas de Lindóia, SP, Brazil

ENCIT-2018-0192
DESIGN AND ANALYSIS OF A SCRAMJET INLET AND COMBUSTION CHAMBER FOR HEAT ADDITION RATE INVESTIGATION

Felipe Jean da Costa
David Romanelli pinto
Instituto Tecnológico de Aeronáutica, Programa de Pós-Graduação em Ciências e Tecnologias Espaciais, Praça Marechal Eduardo Gomes, nž 50 Vila das Acácias CEP. 12.228-900, São José dos Campos, SP, Brasil
felipejean@ieav.cta.br, romanellibr@gmail.com

Gustavo Jean da Costa
Faculdade de Tecnologia de São José dos Campos Prof. Jessen Vidal, Av. Cesare Mansueto Giulio Lattes, nž 1350 Eugênio de Melo CEP. 12.247-014 São José dos Campos, SP - Brasil.
gustavojean15@hotmail.com

Israel da Silveira Rêgo
Antonio Carlos de Oliveira
Tiago Cavalcanti Rolim
Instituto de Estudos Avançados, Divisão de Aerotermodinâmica e Hipersônica,Trevo Coronel Aviador José Alberto Albano do Amarante, nž 1 Putim CEP. 12.228-001, São José dos Campos, SP, Brasil
israel.rego@ieav.cta.br, acoc@ieav.cta.br, tiagotcr@fab.mil.br

Paulo Gilberto de Paula Toro
Universidade Federal do Rio Grande do Norte/UFRN - Centro de Tecnologia. Av. Senador Salgado Filho, 3000 - Campus Universitário, Lagoa Nova CEP 59.078-970 Natal/RN - Brasil
toro@ct.ufrn.br

Abstract. *This work shows preliminary results of the design and analysis of a scramjet inlet and combustor for heat addition rate studies. The inlet was modeled using oblique shockwave equations for a perfect gas and the combustor was assumed to be in chemical equilibrium, considering 10 species. Inviscid flow was assumed. The fuel was hydrogen. The scramjet design Mach number was 7.0 at an altitude of 30 km, with a design fuel equivalence ratio of 0.15. The analysis focuses on how the heat addition rate influences combustor exit temperature, Mach number and geometry. It was found that, independently of the energy added when the flow approaches Mach 1.0, the combustion exit properties values get closer.*

Keywords: *scramjet, Hypersonics, Propulsion, Supersonic Combustion.*

1. INTRODUCTION

Laser energy addition in supersonic combustion has been investigated, in the Prof. Henry T. Nagamatsu Laboratory of Aerothermodynamics and Hypersonics. In the open literature it has been reported the usage of laser energy addition to promote supersonic air mixing with fuel, to improve combustion efficiency and to reduce the ignition time (and consequently the required length for the combustion process), and acting as a flame holder (Brieschenk *et al.*, 2011, 2013). This paper presents a methodology to design a scramjet model (inlet and combustor) for heat addition rate studies in supersonic combustion, considering flight conditions at 30 km altitude at Mach number 7, and the design equivalence ratio was 0.15.

2. METHODOLOGY

TIn the aerodynamic design of the scramjet (Fig.1), we considered the following assumptions: i) in the inlet, air flow with calorically perfect gas behavior, inviscid and adiabatic flow, with oblique shockwave relations, so that the incident shockwave of the compression system focuses in the cowl leading edge (shock-on-lip) and the reflected shockwave focuses at the combustion chamber entrance (shock-on-corner); ii) combustion with constant pressure is considered; iii) combustion process in chemical equilibrium is calculated considering a Gibbs energy minimization process (Gordon and Mcbride, 1994); iv) quasi-one-dimensional inviscid flow in combustor; and v) fuel injection effects were simplified by

using an empirical model to estimate the mixing efficiency (Northam and Anderson, 1986).

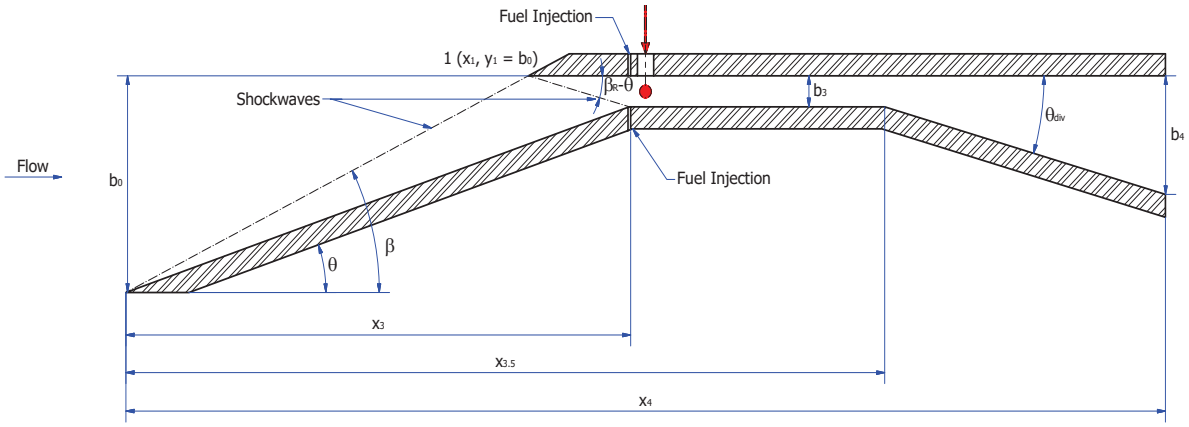

Figure 1: Scramjet scheme for constant pressure combustor.

2.1 Inlet

From the assumptions considered for the inlet, calorically perfect gas, inviscid, two-dimensional and adiabatic flow, we used the oblique shockwave relationships. For the pressure ratio across the shockwave, we have (Anderson, 2007):

$$p_{ratio} = 1 + \frac{2\gamma_0}{\gamma_0 + 1}(M^2_{n,before} - 1) \tag{1}$$

where γ_0 is the ratio of specific heats and $M_{n,before}$ is the upstream normal Mach number.
For the density and velocity ratios:

$$\rho_{ratio} = \frac{1}{u_{ratio}} = \frac{M^2_{n,before}(\gamma_0 + 1)}{2 + (\gamma_0 - 1)M^2_{n,before}} \tag{2}$$

For temperature ratio and specific enthalpy ratios:

$$T_{ratio} = h_{ratio} = p_{ratio}/\rho_{ratio} \tag{3}$$

For the normal Mach number downstream the shockwave we have:

$$M^2_{n,after} = \frac{1 + \frac{(\gamma_0 - 1)}{2} M^2_{n,before}}{\gamma_0 M^2_{n,before} - \frac{(\gamma_0 - 1)}{2}} \tag{4}$$

For the downstream Mach number we have:

$$M_{after} = \frac{M_{n,after}}{sin(\beta - \theta)} \tag{5}$$

Finally, for the shockwave angle β we have:

$$\tan\theta = 2\cot\beta \frac{M^2_{before}\sin^2\beta - 1}{M^2_{before}(\gamma_0 + \cos 2\beta) + 2} \tag{6}$$

where, M_{before} is the upstream Mach number and θ is the local flow deflection. After defining the ramp angle and calculating the shockwave angle, one can obtain the cowl axial position as:

$$x_1 = \frac{b_0}{\tan\beta} \tag{7}$$

And, the axial position of the intersection point between the compression ramp and the oblique shockwave from the reflected flow in the cowl leading edge:

$$x_3 = \frac{b_0 - b_3}{\tan\theta} \tag{8}$$

The ramp length, used in boundary layer analysis, is calculated via:

$$s_3 = \frac{x_3}{\cos\theta} \tag{9}$$

In the equations above, b_0 is given as a function of the combustor height b_3, ramp angle, ramp shockwave angle and the reflected shockwave angle, θ, β and β_R, respectively:

$$b_0 = -b_3 \left[\frac{1}{\tan\theta} + \frac{1}{\tan(\beta_R - \theta)}\right]\left[\frac{1}{\tan\beta} - \frac{1}{\tan\theta}\right]^{-1} \tag{10}$$

To provide an area relief, necessary to avoid thermal choking, we consider that the divergence starts at the theoretical point where ignition starts given by:

$$x_{35} = x_3 + L_i \tag{11}$$

where L_i is the estimated ignition length. The axial position of the combustor exit is given by:

$$x_4 = x_3 + L_c \tag{12}$$

where the total combustor length is determined by:

$$L_c = L_i + L_r + L_{(\eta_{mix}=1)} \tag{13}$$

where L_r is the reaction length, and $L_{(\eta_{mix}=1)}$ is the total mixing length.

2.2 Constant pressure combustor

The conservation equations were applied to the control volume showed in Fig.2 with the assumptions: steady and quasi-one dimensional flow, chemical equilibrium, and neglecting the effects of gravitational, acceleration, electrical, and magnetic fields on the motion or energy of the fluid. For mass conservation we have:

$$\dot{m}_3 + \dot{m}_f = \dot{m}_4 \tag{14}$$

where $\dot{m}_f$ is the fuel mass flow rate. For momentum conservation in the axial direction:

$$p_3 A_3 + \dot{m}_3 u_3 + \dot{m}_f u_f + F_x = p_4 A_4 + \dot{m}_4 u_4 \tag{15}$$

For energy conservation:

$$\dot{m}_3\left(h_3 + \frac{u_3^2}{2}\right) + \dot{m}_f\left(h_f + \frac{u_f^2}{2} + \frac{v_f^2}{2}\right) + \dot{W} + \dot{Q} = \dot{m}_4\left(h_4 + \frac{u_4^2}{2}\right) \tag{16}$$

The total rate of heat added is given by:

$$\dot{Q} = \dot{Q}_{visc} + P_{ext} \tag{17}$$

where $\dot{Q}_{visc}$ is the heat transfer rate due to the viscous effects, and P_{ext} is the rate of heat added by an external source. We assume the total axial force applied to the control volume is equal to the viscous forces, which can be estimated by:

$$F_x = -\tau_w S_w \tag{18}$$

where τ_w is the wall shear stress (estimated via the skin friction coefficient), and S_w is the combustor wetted area. From the geometry given by Fig. 2, the wetted area is given by:

$$S_w = \frac{2L_i A_3}{w} + L_i w + L_c w + (L_c - L_i)\frac{A_3 + A_4}{w} + \frac{L_c - L_i}{w\cos\theta_{div}} \tag{19}$$

where w is the combustor width and θ_{div} is the divergence angle.

With the assumption of a constant pressure combustion $p_4 = p_3$, one can obtain the combustor exit velocity after some algebraic manipulation of Eq. (15):

$$u_4 = \frac{1}{\dot{m}_4}\left(F_x + A_3 p_3 + \dot{m}_3 u_3 + \dot{m}_f u_f - A_4 p_4\right) \tag{20}$$

For the density at station 4 one may calculate it by:

$$\rho_4 = \frac{\dot{m}_4}{u_4 A_4} \tag{21}$$

From the energy conservation, Eq. (16), considering no work is done by the fluid $\dot{W} = 0$, one can solve for the specific enthalpy at combustor exit:

$$h_4 = \frac{1}{\dot{m}_4}\left[\dot{m}_3\left(h_3 + \frac{u_3^2}{2}\right) + \dot{m}_f\left(h_f + \frac{u_f^2 + v_f^2}{2}\right) + \dot{Q}\right] - \frac{u_4^2}{2} \tag{22}$$

In the numerical procedure, the objective was to find zero of the error function defined by:

$$\epsilon = h_4 - h(p_4, \rho_4, \phi_0) \tag{23}$$

by varying A_4. The tolerances were 10^{-3} J/kg for the error function and 10^{-9} m^2 for the area. The specific enthalpy $h(p_4, \rho_4, \phi_0)$ is calculated considering chemical equilibrium based on Gibbs energy minimization, the considered species were $N_2, H_2O, O_2, H_2, OH, H, O, Ar, NO$ and N. The thermodynamic properties of each species were calculated using the NASA polynomials (Gordon and Mcbride, 1994) with updates of the coefficients provided by Burcat and Ruscic (2005). After this procedure one can calculate the combustor divergence angle by:

$$\theta_{div} = \tan^{-1}\left(\frac{\frac{A_4 - A_3}{w}}{L_c - L_i}\right) \tag{24}$$

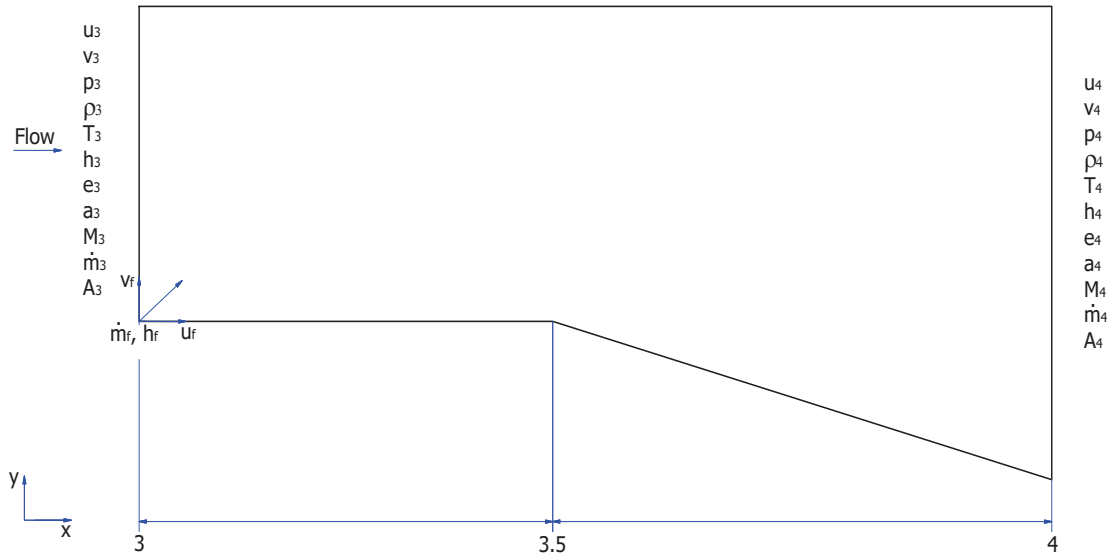

Figure 2: Combustor control volume for constant pressure.

2.3 Sonic conditions

As written above, the set of equations, Eq. (20) to Eq. (24) is unable to find the conditions at Mach 1.0, $u_4 = a_4$. Thus, another equation must be added:

$$\xi = u_4 - a_4 \tag{25}$$

which was solved with a precision of 10^{-3} m/s.

2.4 Boundary-layer

To account for the boundary-layer effects, we used the Simeonides model (Simeonides, 1990), considering a turbulent flow over a flat plate. In this model, the skin friction coefficient is given by:

$$c_f = \frac{0.0592}{Re_s^{1/5}}\left(\frac{T}{T^*}\right)^{4/5}\left(\frac{\mu^*}{\mu}\right)^{1/5} \tag{26}$$

Using the reference temperature concept (Weiland and Hirschel, 2009),

$$T^* = 0.28T + 0.5T_w + 0.22T_{aw} \tag{27}$$

where:

$$T_{aw} = T\left(1 + r\frac{\gamma_0 - 1}{2}M^2\right) \tag{28}$$

For turbulent flow the recovery factor r becomes (Schlichting, 1979):

$$r = \mathrm{Pr}^{1/3} \tag{29}$$

where Pr = 0.71 (Anderson, 2007). The Reynolds number is calculated with:

$$Re_s = \frac{\rho u s}{\mu} \tag{30}$$

where s is a coordinate tangential to the compression ramp surface. We used the Sutherland's law to calculate viscosities (Weiland and Hirschel, 2009):

$$\mu = 1.458 \cdot 10^{-6}\frac{T^{1.5}}{T + 110.4} \tag{31}$$

,

$$\mu^* = 1.458 \cdot 10^{-6}\frac{T^{*1.5}}{T^* + 110.4} \tag{32}$$

We evaluated Eqs. (26) through (32) at station 3, where, as a design option, we considered $T_w = 800$ K (constant along the inlet) and we assumed that the wall shear stress is constant along the combustor, so that it can be calculated by the relation:

$$\tau_w = \frac{1}{2}\rho_3 u_3^2 c_f \tag{33}$$

Following, according to Simeonides (1990), the heat flux is calculated by:

$$\dot{q}_w = S_t \rho u \left(h_{aw} - h_w\right) \tag{34}$$

which was also evaluated at station 3, according to our assumption. The Stanton number is estimated by means of a Reynolds analogy:

$$S_t = c_f/2 \tag{35}$$

So the heat added by the viscous effects may be expressed by:

$$\dot{Q}_{visc} = \dot{q}_w S_w \tag{36}$$

However, in order to simplify the calculations and since we are emphasizing the effects of the heat addition rate on the flow in the combustor, we considered adiabatic wall condition $h_w = h_{aw}$, so $\dot{Q}_{visc}$ = 0.

2.5 Fuel-air mixture

The fuel and air mass flow ratio f, or fuel-air ratio, is a general indicator of the combustor process (Heiser *et al.*, 1994). The fuel-air ratio is given by:

$$f = \frac{\dot{m}_f}{\dot{m}_0} \tag{37}$$

The stoichiometric value of f, or the ideal fuel-air ratio named f_{st} is related with a greater energy release in the combustion, and if one consider a hydrocarbon complete combustion reaction (without Argon)(Heiser *et al.*, 1994):

$$C_x H_y + \left(x + \frac{y}{4}\right)\left(O_2 + \frac{79}{21}N_2\right) \rightarrow xCO_2 + \frac{y}{2}H_2O + \frac{79}{21}\left(x + \frac{y}{4}\right)N_2 \tag{38}$$

One can calculate the general expression for the stoichiometric fuel-air ratio, considering the atomic weight of the elements, by:

$$f_{st} = \frac{36x + 3y}{103(4x + y)} \tag{39}$$

For hydrogen $f_{st} = 0.0291$. Another important parameter for the combustion is the equivalence ratio ϕ_0, that allows to quantify the amount of fuel injected and it is defined by:

$$\phi_0 = \frac{f}{f_{st}} \tag{40}$$

With the equivalence ratio one can determine if the mixture is rich or poor in fuel: when $\phi_0 < 1$ the mixture is poor, in other hand, when $\phi_0 > 1$ the mixture is rich.

2.6 Fuel-air mixing model

For the fuel-air mixing model, we use the concept of mixing efficiency with the methodology adopted by Northam and Anderson (1986). The mixing efficiency is defined as the ratio between the amount of fuel available for the reaction and the total amount of fuel injected. Based on experimental data, the mixing efficiency is a function of the axial distance and the required distance for complete mixing of the reactants. The mixing efficiency for axial injection may then given as:

$$\eta_{mix,0^o} = \frac{x}{L_{(\eta_{mix}=1)}} \tag{41}$$

In the case of normal fuel injection, we have:

$$\eta_{mix,90^o} = 1.01 + 0.176ln\frac{x}{L_{(\eta_{mix}=1)}} \tag{42}$$

In this mixing model, once the values of the mixing efficiency for axial and normal cases are known, one can obtain the values for injection angles between $0^o - 90^o$, applying a linear interpolation.

$$\frac{L_{(\eta_{mix}=1)}}{b_3} = \begin{cases} 0.179C_{mix}e^{1.72\phi_0}, & \phi_0 \leq 1 \\ 3.333C_{mix}e^{-1.204\phi_0}, & \phi_0 > 1 \end{cases} \tag{43}$$

given that b_3 is the height of the combustor entrance and C_{mix} is an empirical constant of mixing rate. In this work, it was considered $C_{mix} = 47$ as suggested by Pulsonetti, Erdos and Early Pulsonetti *et al.* (1991).

2.7 Ignition and reaction times and estimation of the combustor length

According to Paull and Stalker (2000), there are four parameters that must be known for the occurrence of self-ignition and subsequent combustion, they are the static temperature, the static pressure, the fuel-air mixture, and residence time. Thus, we can define the ignition time t_i as the necessary time from ignition until 95% of the heat is released via the formation of products, in this case H_2O. The ignition time is given by:

$$t_i = \frac{8 \times 10^{-9} e^{\frac{9600}{T}}}{p} \tag{44}$$

in this relation, p is in atm and T in K. Similarly, the reaction time can be estimated by

$$t_r = \frac{1.05 \times 10^{-4} e^{\frac{-1.12T}{1000}}}{p^{1.7}} \tag{45}$$

In this work, the necessary length for ignition and reaction processes are estimated by:

$$L_i = u_3 t_i \tag{46}$$

and

$$L_r = u_3 t_r \tag{47}$$

3. RESULTS AND DISCUSSIONS

3.1 Chemical equilibrium validation

It was conducted an analysis for the chemical equilibrium validation between the developed code and NASA CEA code (Gordon and Mcbride, 1994). The conditions were pressure of 1.0 atm with equivalence ratios of 1.0 and 0.5. The temperature varied from 600 to 5000 K. The results are presented in the Fig. 3. The presented results indicate that the developed code have almost identical values compared with those from the NASA CEA code for all species. The considered species were $N_2, H_2O, O_2, H_2, OH, H, O, Ar, NO$ and N.

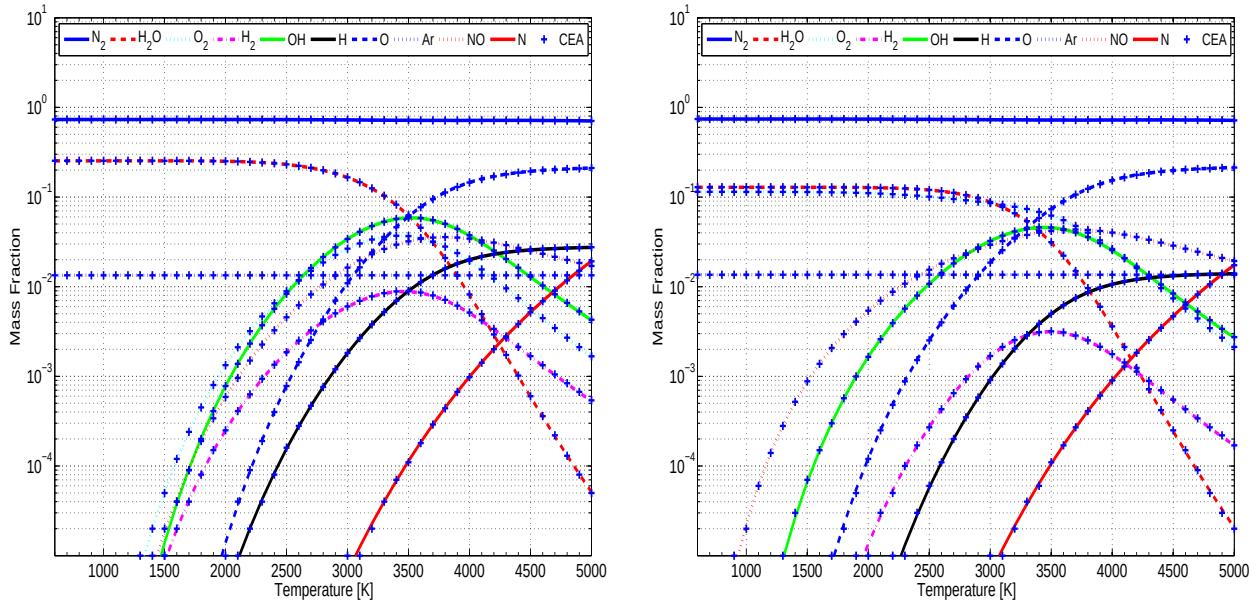

(a) Equivalence ratio of 1.0 (b) Equivalence ratio of 0.5

Figure 3: Comparisons with NASA CEA code, pressure of 1.0 atm and equivalence ratios of 1.0. and 0.5.

3.2 Combustor Exit Properties

The analysis was carried on with the heat addition rate varying from 0 to 10^6 W, and the equivalence ratio varying from 0.1 to 1.0. However, for the heat addition rate of 10^6 W all cases presented thermal choking ($M_4 \leq 1.0$) and in this case, the calculation stops because only supersonic flow was considered, this fact also limits the equivalence ratio. In Fig. 4a, one can see the variation of the combustor exit temperature with the equivalence ratio up to choking condition for several values of the heat addition rate (0, 10, 10^2, 10^3, 10^4 and 10^5 W). The temperature is increased with the increase of equivalence ratio because more chemical energy is available to be converted in internal energy. It can be noted an almost linear variation for all values of the heat addition rate, with the results very close together when the heat addition rate varied from 0 to 10^4 W, however, for 10^5 W the combustor exit temperature values were pronounced higher. With no heat addition rate (0 W), the combustor exit temperature reaches 1455 K at ϕ_0 = 0.1 and 2579 K as final value. Considering the heat addition rate 10^5 W we have the combustor exit temperature of 1702 K at ϕ_0 = 0.1 and 2609 K as final value. The relative difference between the maximum and minimum values of the combustor exit temperature with no heat addition rate (0 W) is 77.19 %, and 53.28 %, considering the maximum heat addition rate of 10^5 W. According to the graph, Fig. 4b, the Mach number sensibly decreases from 2.11 to 1.00 considering no heat addition rate (0 W), while considering the heat addition rate 10^5 W the Mach number decreases from 1.89 to 1.00, approaching to the thermal choking due to the increase of the speed of sound with the temperature augmentation. Indeed, the curve of Mach number variation was almost the inverse of the temperature variation curve, Fig. 4a.

In Fig.5a with no heat addition rate (0 W) the minimum area ratio A_4/A_3 was 1.47 and the maximum was 4.61. Considering the heat addition rate of 10^5 W we have the minimum area ratio equal to 1.78 and maximum equal to 4.62. The area is increased due to the constant pressure assumption, however, the area change does not avoid near thermal choking condition, when the heat addition rate was zero the maximum equivalence ratio was 0.525 and when the heat addition rate was 10^5 W the equivalence ratio was 0.466 when $M_4 = 1.0$. In practical terms, the area increase is related to the divergence angle (θ_{div}) defined in the Fig. 1 and presented in Fig. 5b, where the minimum divergence angle of the combustor was 1.42 deg. and the maximum was 10.86 deg., considering no heat addition rate. Applying the heat addition rate of 10^5 W, the minimum divergence angle of the combustor was 2.38 deg. and the maximum was 10.87 deg.

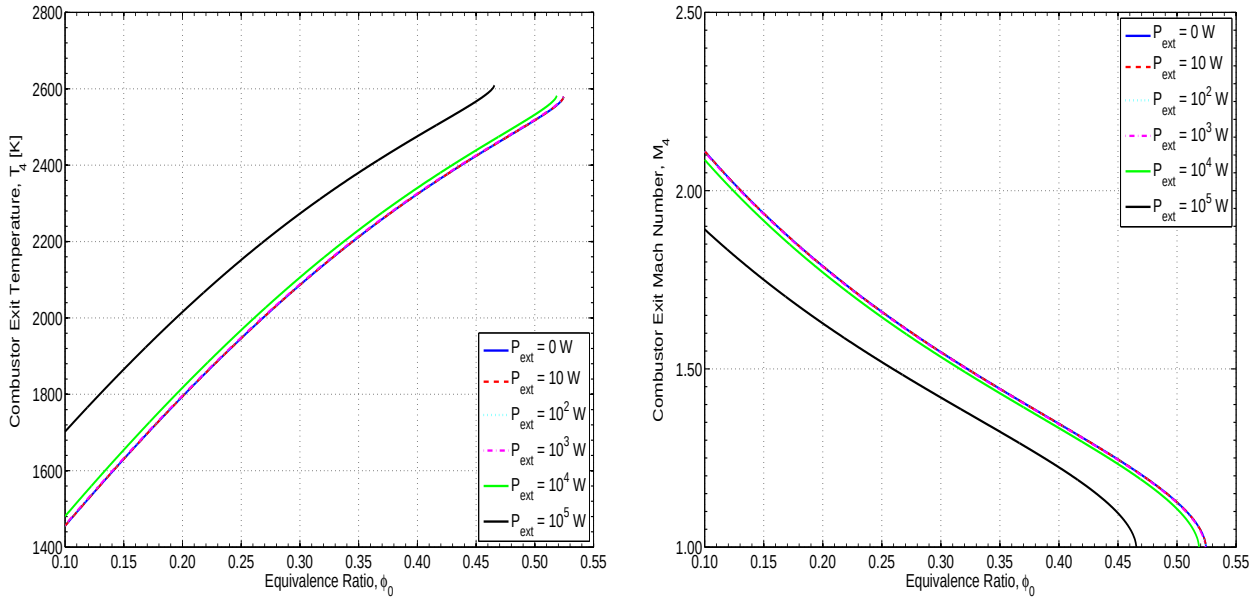

(a) Combustor exit temperature (T_4)

(b) Combustor exit Mach number (M_4)

Figure 4: Combustor exit temperature and Mach number as function of the equivalence ratio (ϕ_0 varying from 0.10 to 0.525) and heat addition rate (varying from 0 to 10^5W).

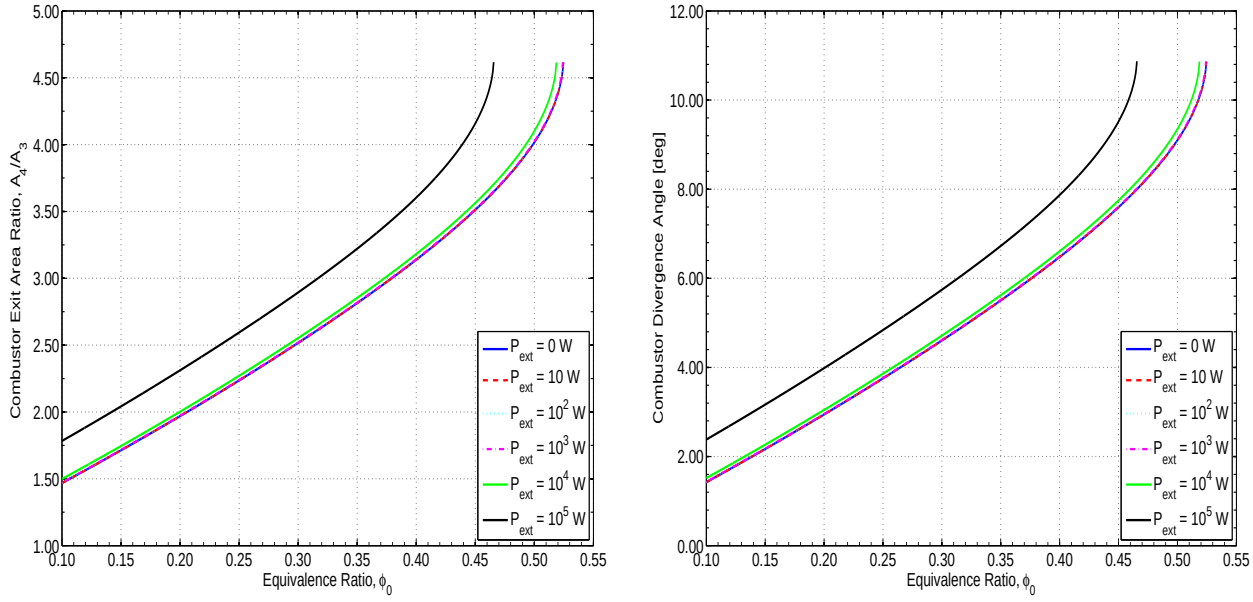

(a) Combustor area ratio (A_4/A_3)

(b) Combustor divergence angle (θ_{div})

Figure 5: Area ratio and combustor divergence angle as functions of the equivalence ratio (ϕ_0 varying from 0.1 to 0.525) and heat addition rate (varying from 0 to 10^5W).

An important remark is that independently of the added energy, when the flow approaches to Mach 1.0, the combustion exit properties values get closer.

4. CONCLUSIONS

This work shows the preliminary results from the design and analysis of a scramjet inlet and combustor for heat addition rate studies. The design presented in this paper covers the main methodologies for the development of a scramjet engine from inlet to combustor. The results were presented firstly by showing the validation of the chemical equilibrium methodology used on the developed code with the NASA CEA Code. Secondly, we evaluated the heat addition rate influence on the key properties considering constant pressure combustor with a viscous flow approach. From this study, we could conclude that the heat addition rate produces higher combustor exit temperatures, divergence angles and exit pressures. On other hand, it causes a decrease in the combustor exit Mach number. It was also noted that the heat addition rate causes an early thermal choking at the combustor.

5. ACKNOWLEDGMENTS

This work was supported by the COMAER PROPHIPER 14-X project, Instituto de Estudos Avançados and Instituto Tecnológico de Aeronáutica.

6. REFERENCES

Anderson, J.D., 2007. *Fundamentals of Aerodynamics*. McGraw-Hill, London, UK, 4th edition.

Brieschenk, S., Byrne, S.O. and Kleine, H., 2011. "Laser-Induced Plasma Ignition Experiments in a Scramjet Inlet". *AIAA 2011-504*.

Brieschenk, S., Byrne, S.O. and Kleine, H., 2013. "Laser-induced plasma ignition studies in a model scramjet engine". *Combustion and Flame*, Vol. 160, No. 1, pp. 145–148. ISSN 0010-2180. doi:10.1016/j.combustflame.2012.08.011. URL `http://dx.doi.org/10.1016/j.combustflame.2012.08.011`.

Burcat, A. and Ruscic, B., 2005. "Third Millennium Ideal Gas and Condensed Phase Thermochemical Database for Combustion with Updates from Active Thermochemical Tables". Technical report, Argonne.

Gordon, S. and Mcbride, B.J., 1994. "Computer Program for Calculation of Complex Chemical Equilibrium Compositions and Applications I. Analysis". RP 1311, NASA.

Heiser, W.H., Pratt, D.T., Daley, D.H. and Mehta, U.B., 1994. *Hypersonic Airbreathing Propulsion*. AIAA Education Series. AIAA, Washington, DC. doi:10.2514/4.470356.

Northam, G.B. and Anderson, G.Y., 1986. "Survey of Supersonic Combustion Ramjet at Langley". *AIAA 86-0159*.

Paull, A. and Stalker, R.J., 2000. *Scramjet Testing in the T3 and T4 Hypersonic Impulse Facilities*, Vol. 189. ISBN 1-56347-322-4. doi:10.2514/5.9781600866609.0001.0046.

Pulsonetti, M.V., Erdos, J. and Early, K., 1991. "Engineering Model for Analysis of Scramjet Combust or Performance with Finite-Rate Chemistry". *Journal of Propulsion and Power*, Vol. 7, No. 6, pp. 1055–1063.

Schlichting, H., 1979. *Boundary-Layer Theory*. McGraw-Hill Series in Mechanical Engineering, New York, NY.

Simeonides, G., 1990. "THE VKI HYPERSONIC WIND TUNNELS and ASSOCIATED MEASUREMENT TECHNIQUES". Technical Report November, Von Karman Institute.

Weiland, C. and Hirschel, E., 2009. *Selected Aerothermodynamic Design Problems of Hypersonic Flight Vehicles*. Progress in Astronautics and Aeronautics. American Institute of Aeronautics and Astronautics, Inc., Washington, DC. ISBN 978-1-56347-990-8. doi:10.2514/4.479908. URL `http://arc.aiaa.org/doi/book/10.2514/4.479908`.

7. RESPONSIBILITY NOTICE

The author(s) is (are) the only responsible for the printed material included in this paper.